HHS Public Access

Author manuscript

J Control Release. Author manuscript; available in PMC 2019 January 28.

Published in final edited form as:

J Control Release. 2018 January 28; 270: 14–22. doi:10.1016/j.jconrel.2017.11.028.

RNA Nanoparticle Distribution and Clearance in the Eye after Subconjunctival Injection with and without Thermosensitive Hydrogels

Zhanquan Shi[a], **S. Kevin Li**[a,*], **Ponwanit Charoenputtakun**[a,b], **Chia-Yang Liu**[c,d], **Daniel Jasinski**[e], and **Peixuan Guo**[e]

[a]Division of Pharmaceutical Sciences, James L. Winkle College of Pharmacy, University of Cincinnati, Cincinnati, OH 45267 [b]Pharmaceutical Development of Green Innovations Group (PDGIG), Faculty of Pharmacy, Silpakorn University, Nakhon Pathom, Thailand [c]Department of Ophthalmology, College of Medicine, University of Cincinnati, Cincinnati, OH 45267 [d]School of Optometry, Indiana University, Bloomington, IN 47405 [e]College of Pharmacy, Division of Pharmaceutics and Pharmaceutical Chemistry; College of Medicine, Department of Physiology & Cell Biology; and Dorothy M. Davis Heart and Lung Research Institute; Complehensive Cancer Center; and Center for RNA Nanobiotechnology and Nanomedicine, The Ohio State University, Columbus, Ohio, USA

Abstract

Thermodynamically and chemically stable RNA nanoparticles derived from the three-way junction (3WJ) of the pRNA from bacteriophage phi29 DNA packaging motor were examined previously for ocular delivery. It was reported that RNA nanoparticles with tri-way shape entered the corneal cells but not the retinal cells, whereas particle with four-way shape entered both corneal and retinal cells. The present study evaluated ocular delivery of RNA nanoparticles with various shapes and sizes, and assessed the effect of thermosensitive hydrogels (poly(lactic-co-glycolic acid)-b-poly(ethylene glycol)-b-poly(lactic-co-glycolic acid); PLGA-PEG-PLGA) for increasing the retention of RNA nanoparticles in the eye. Fluorescence imaging of mouse eyes and fluorescence microscopy of dissected eye tissues from the conjunctiva, cornea, retina, and sclera were performed to determine the distribution and clearance of the nanoparticles in the eyes after subconjunctival injection *in vivo*. RNA nanoparticles entered the cells of the conjunctiva, cornea, retina, and sclera after subconjunctival delivery. The clearance of RNA pentagon was slower than both RNA square and triangle of the same designed edge length (10 nm) in the eye, and the clearance of RNA squares of the longer edge lengths (10 and 20 nm) was slower than RNA square of the shorter edge length (5 nm), thus indicating that the size could affect ocular pharmacokinetics of the nanoparticles. At 24 h after the injection, approximately 6–10% of the

*Corresponding author: Address: College of Pharmacy, 231 Albert Sabin Way, MSB # 3005, Cincinnati, OH 45267-0514, USA, Tel: (513) 558-0977, kevin.li@uc.edu.

fluorescence signal from the larger nanoparticles in the study (RNA square of 20 nm edge length and RNA pentagon of 10 nm edge length) remained in the eye, and up to 70% of the retinal cells contained the nanoparticles. The results suggest that the larger nanoparticles were “gulped” in conjunctival, corneal, retinal, and scleral cells, similar to the behavior observed in macrophages. Additionally, the combination of RNA nanoparticles with the thermosensitive polymers increased the retention of the nanoparticles in the eye.

Graphical abstract

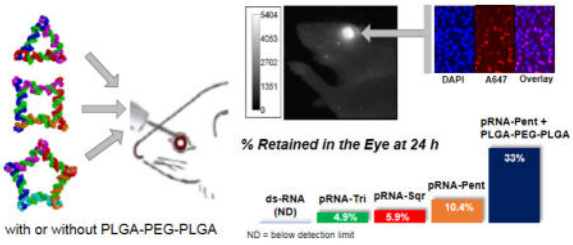

Keywords

RNA nanoparticle; double-stranded RNA; temperature sensitive polymer; subconjunctival; ocular delivery

1. Introduction

The increasing interest in RNA therapeutics has led to the rapid emergence of the field of RNA nanotechnology [1–3], a concept that was proved in 1998 when it was found that RNA dimer, trimer, tetramer, and hexamer can be produced via bottom-up assembly of fabricated RNA fragments derived from the packaging RNA (pRNA) subunit of phi29 DNA packaging motor [4]. One recent advancement in RNA nanotechnology is the integration of multiple functional modules for targeting, therapy, and detection into one RNA nanoparticle. The nanoparticle derived from the three-way junction (3WJ) of the pRNA of bacteriophage phi29 DNA packaging motor has recently shown great promise for the delivery of multiple functional units [4–7]. This unique RNA nanotechnology approach is different from the traditional conjugation of siRNA/miRNA to nanoparticles for drug delivery [8]. Recently, the 3WJ has been used as a module for the construction of diverse size and shape RNA nanoparticles [7, 9]. The following are the advantages of using RNA nanoparticles in drug delivery [7–10]. RNA nanoparticles with defined size, shape, and stoichiometry can be constructed to allow simultaneous targeting and/or delivery of multiple therapeutic and targeting ligands for achieving synergistic effects. These nanoparticles with the 3WJ as the scaffold are thermodynamically stable at ultra-low concentrations in the body, chemically resistant to RNase degradation in blood after chemical modifications, and nontoxic. The RNA nanoparticles can be made to avoid interferon induction, cytokine production, and host immune responses in animals, or they can be made highly active in stimulating cytokine induction for vaccine adjuvant and cancer immunotherapy, depending on the tunable shapes and sequences. Despite the advantages, these RNA nanoparticles have not been studied extensively for ocular drug delivery.

Effective ocular drug delivery to treat chronic posterior eye diseases remains a challenging task [11, 12]. These treatments require repeated intravitreal injections and involve high healthcare cost, and repeated ocular perforation can lead to adverse effects such as intraocular bleeding, infection, and retinal detachment [13]. A more effective system for drug delivery to the posterior segment of the eye is desirable. For example, subconjunctival injection does not perforate the eyeball and is considered safer with less serious complications than intravitreal injection. A recent study has evaluated the distribution of RNA nanoparticles in the eye after topical and subconjunctival administrations for their potential in ocular delivery [14]. Two types of RNA nanoparticles were investigated: the three-way junction (pRNA-3WJ) and its four-way X-shape extension (pRNA-X). After subconjunctival injection of the RNA nanoparticles, the nanoparticles were found in the cells of the cornea for up to 20 h, but only pRNA-X was internalized in the cells in the retina. The number of cells in the retina with pRNA-X internalization also decreased rapidly and was not present in the tissue at 12 h after the injection. This was the first study of RNA nanoparticles in ocular delivery and the first time that nanoparticles were found in retinal cells after subconjunctival injection without physical or chemical penetration enhancement methods. As the understanding of RNA nanoparticle delivery and clearance in the eye is essential in the development of this new system for ocular drug delivery, the next logical step is to evaluate the effects of the particle sizes of these nanoparticles on ocular pharmacokinetics.

Due to the observed fast clearance and elimination of the RNA nanoparticles from the eye after subconjunctival injection, the development of a sustained release system to prolong transscleral delivery of the RNA nanoparticles from the subconjunctival space is essential for long term treatment of posterior eye diseases via the subconjunctival route. The sol-gel system is a temperature sensitive polymer system that is in liquid state at room temperature for the injection and becomes a gel in the subconjunctival space at body temperature after the injection [15]. An example is the temperature sensitive PLGA-PEG-PLGA triblock copolymer systems [16, 17]. A previous study has suggested the use of PLGA-PEG-PLGA sol-gel system to decrease conjunctival clearance and provide sustained drug delivery from the subconjunctival pocket after subconjunctival administration [18]; this was one of the first studies to evaluate the sol-gel system in ocular drug delivery, and to our knowledge, the only study of PLGA-PEG-PLGA hydrogel in subconjunctival delivery (of dexamethasone). The hypothesis in the present study was that a thermosensitive hydrogel could increase the residence time of RNA nanoparticles in the eye to prolong ocular delivery of the RNA nanoparticles after subconjunctival administration.

As a continuing effort to examine the feasibility of using RNA nanoparticles for drug delivery to the posterior eye via subconjunctival injection and to improve ocular delivery of these nanoparticles, the objectives of the present study were to (a) evaluate the distribution and clearance of RNA nanoparticles of various shapes (triangular, square, and pentagonal RNA nanoparticles: pRNA-Tri, pRNA-Sqr, and pRNA-Pent, respectively) of the same and different designed edge lengths (lengths along each edge, Fig. 1A) in the eye after subconjunctival injection; (b) compare the results of these RNA nanoparticles to those of pRNA-3WJ and pRNA-X in the previous study; and (c) examine the feasibility of sol-gel polymers to prolong the delivery of pRNA via the subconjunctival route. PLGA-PEG-PLGA

triblock copolymers were the sol-gel systems investigated. The hypotheses were that (a) these nanoparticles with similar constructs as pRNA-X could be delivered to the retina after subconjunctival injection, and with their larger sizes, could provide longer retention in the eye tissues than pRNA-X and (b) the sol-gel polymers could further extend the half-lives of these nanoparticles in the eye. Fluorescence imaging of the eyes using the whole-body imaging technique was performed in mice to determine the pharmacokinetics and clearance of the nanoparticles in the eyes after subconjunctival injection *in vivo*. Fluorescence microscopy using the confocal technique was performed on dissected eye tissues obtained at predetermined time points after subconjunctival injection *in vivo* to examine the distribution of nanoparticles to the ocular tissues. To our knowledge, this is the first study to evaluate RNA nanoparticles of different shapes for ocular drug delivery via subconjunctival injection. It is also the first to use PLGA-PEG-PLGA hydrogel in subconjunctival delivery of nanoparticles.

2. Material and methods

2.1. Animals and reagents

Adult mice of approximately 8 weeks old (SKH1 and C57BL/6 strains) were purchased from Charles River Laboratories International (Wilmington, MA). All animal experiments were carried out in compliance with the Association for Research in Vision and Ophthalmology (ARVO) Statement for the Use of Animals in Ophthalmic and Vision Research, and with the approval of the Institutional Animal Care and Use Committee (IACUC) at the University of Cincinnati.

Alexa-647 (A647) labeled RNA nanoparticles of pRNA-Tri, pRNA-Sqr, pRNA-Pent, and pRNA-X were synthesized as described previously [5, 7, 9]. The RNA nanoparticles contained 2′-F U and C nucleotides to make them resistant to RNase degradation. Alexa-647 labeled double-stranded RNA (ds-RNA) of 16 bp was synthesized using the same procedure. All nanoparticles were stored at stock concentration of 10 or 15 μM in TMS buffer (TRIS-HCl 50 mM, pH 8.0, 100 mM NaCl, and 10 mM $MgCl_2$) in a −20°C freezer before use. RNA nanoparticle solutions for the injection were prepared freshly before the experiment by the dilution of the nanoparticle stock solution with phosphate buffered saline (PBS) to a working concentration of 2.5 μM. Alexa-647 dye was purchased from Life Technologies Corp. (Grand Island, NY) and stored at stock concentration of 100 μM. Tri-block copolymers AK24 and AK97 were purchased from Polyscitech (West Lafayette, IN). AK24 is PLGA-PEG-PLGA of LA:GA 3:1 (w:w) and Mn ~1,100:1,000:1,100 Da, and AK97 is PLGA-PEG-PLGA of LA:GA 15:1 (w:w) and Mn ~1,700:1,500:1,700 Da. PBS solution was prepared by dissolving PBS tablets (MP Biomedicals, LLC, Solon, OH) in deionized water. 4% paraformaldehyde (PFA) was prepared by PFA powder and PBS, and its pH was adjusted to pH 7.4. 4,6-Diamdino-2-phenylindole (DAPI) was purchased from Sigma-Aldrich (St. Louis, MO). Xylazine and ketamine were from Phoenix Pharmaceuticals (St. Joseph, MO).

2.2. Subconjunctival injection in mice

SKH1 hairless mice were used in the pharmacokinetic study of whole-body fluorescence imaging, and C57BL/6 mice were used in the distribution study of fluorescence microscopy. In the imaging study, the mice were anesthetized by 2% isoflurane. In the fluorescence microscopy study, the animals were anesthetized by intraperitoneal (*i.p.*) injection of 10 mg/kg xylazine and 80 mg/kg ketamine in PBS. Under anesthesia, the mouse conjunctiva was slightly pull from the sclera by a pair of fine forceps, and 10 μl of RNA nanoparticle solution or reference solution of ds-RNA or Alexa-647 dye was injected in the superior subconjunctival region by a microsyringe with 33G needle under an anatomical microscope.

2.3. Pharmacokinetics of pRNA-Tri, pRNA-Sqr, and pRNA-Pent in the eye after subconjunctival injection

The clearance of pRNA-Tri, pRNA-Sqr, and pRNA-Pent of 10 nm edge length and pRNA-Sqr of 5 and 20 nm edge lengths in the eye was evaluated after subconjunctival injection of 10 μl 2.5 μM RNA nanoparticles in PBS *in vivo*. Immediately after the injection, the eye surface was cleaned by cotton tips gently. The mice were anesthetized with 2% isoflurane for the injection and during imaging and were put back in their cages after each image acquisition. Whole-body fluorescence images of the eyes were captured using Bruker *In-Vivo* Multispectral Imaging System FX (MS FX Pro) with Carestream Molecular Imaging (MI) software version 5.0.7.24 (Rochester, NY) at time points of 0, 0.5, 1, 2, 4, 6, 9, 12, 48, and 72 h after the injection. Three imaging protocols were used: surface optical imaging for 0.175 s exposure time; fluorescence imaging at 630 nm excitation and 700 nm emission, 10 s exposure time, F-stop 2.51, to detect Alexa-647 signal; and X-ray, F-stop 3.99, 30 s exposure, for anatomical reference. All three protocols used the same field of view (FOV) of 80 mm × 80 mm. A small volume of known concentration of Alexa-647 dye in a clear centrifuge tube was also measured at different time points as a reference. Background fluorescence signals of mouse eyes were measured before the experiment and the average was used to calculate the net signal strength. Subconjunctival injections of ds-RNA and Alexa-647 dye were used as references. In data analysis, the fluorescence images were overlaid on corresponding anatomical reference images. The images were exported into 32-bit integer raw format and analyzed by Image J (ver. 1.49t). Mean fluorescence intensity of the region of interest (ROI) that covered the eye was calculated. The signal strength was reported as percent of signal intensity at the time point to that of zero time point intensity. The data were analyzed using a biphasic first-order clearance kinetics model:

$$C = Ae^{-kt} + Be^{-k't} \quad (1)$$

where C is the signal intensity representing the concentration of the drug remaining in the eye at time t, A and B are constants, and k and k' are the apparent rate constants of the fast and slow elimination phases, respectively. In these analyses, the rate constant of the initial fast elimination phase was determined in the early time period assuming that the contribution from the slow elimination phase was small.

2.4. Distribution of pRNA-Tri, pRNA-Sqr, and pRNA-Pent in the eye after subconjunctival injection

Distribution of pRNA-Tri, pRNA-Sqr and pRNA-Pent of 10 nm edge length was examined by fluorescence microscopy of the dissected eyes after subconjunctival injection of 10 μl 2.5 μM RNA nanoparticles in PBS *in vivo* using the method similar to that in a previous study [14]. Briefly, the animals were sacrificed at 6, 12, 24, 36, and 48 h after the injection. After animal euthanasia, the eye including the conjunctiva and eyelids were collected immediately and rinsed in PBS for 2X 30 min at room temperature to remove blood and potential contaminations. The eye samples were fixed in 4% PFA at 4°C for 2–3 h, followed by 3X 10 min rinsing in PBS. Then, tissues of conjunctiva, cornea, retina, and sclera were isolated, and stained with 0.01% DAPI overnight at room temperature, avoiding any light exposure. The sclera tissue was comprised of the retina pigment epithelium (RPE) and sclera. Each tissue was mounted on a microscope slide with cover glass using a method similar to that of whole mount confocal fluorescence microscopy [19, 20] and analyzed by grid projection microscopy (apotome fluorescence microscopy).

Images of the RNA nanoparticles in the tissues at the 6, 12, 24, 36, and 48 h time points were taken using Carl Zeiss AxioCam Observer Z1 fluorescence microscope with AxioVision SE64 Rel. 4.8 analytical system (Carl Zeiss Microscopy, LLC, Thornwood, NY). Tissues were imaged at wavelength of 461 nm for DAPI and 665 nm for Alexa-647. At least five images in different areas were taken for each tissue to ensure that there was no bias in the analysis. Images were analyzed using software AxioVision LE6.4. Analyses were performed by counting the Alexa-647 stained cells and total number of cells stained by DAPI in Image J: all positively DAPI stained cells with clear outline were counted, and Alex-647 with shapes that matched with the DAPI stained cells were counted. The percent of Alexa-647 stained cells to the DAPI stained cells was then calculated. Subconjunctival injections of pRNA-X, ds-RNA, and Alexa-647 dye, which was studied previously, were used as the references in this study. Images of tissues from PBS injection (without RNA nanoparticles) were the background control.

2.5. Evaluation of thermosensitive tri-block copolymer PLGA-PEG-PLGA for ocular pRNA delivery

The tri-block PLGA-PEG-PLGA copolymers AK24 and AK97 were dissolved in PBS at 4°C or room temperature to prepare 20% AK24, AK97, and 1:1 mixture of AK24 and AK97 polymer solutions. The polymer solutions were stored in a −20°C freezer before use. The liquid-to-gel transition temperatures of AK24, AK97, and 1:1 mixture of AK24 and AK97 were determined by physical observation of 0.2 ml 16.7% polymer solution each in a small glass tube, which had the same concentration as that in the *in vivo* studies in Section 2.6. The glass tube was first put in ice cold water. Then, the temperature of water was increased slowly (e.g., at a rate of ~1°C every several minutes) using a water-bath and the physical behavior of the solution was monitored.

2.6. Pharmacokinetics of pRNA-Pent in the eye after subconjunctival injection with PLGA-PEG-PLGA

Based on the results of pRNA-Tri, pRNA-Sqr, and pRNA-Pent in PBS, which showed the percent of pRNA-Pent (10 nm edge length) in the eye at 24 h was among the highest of the RNA nanoparticles studied in the pharmacokinetic imaging and distribution microscopy studies (see Sections 3.1 and 3.2), pRNA-Pent was selected for the polymer studies. In the experiments, pRNA-Pent was mixed with 20% AK24, AK97, or 1:1 mixture of AK24 and AK97 stock polymer solution to obtain final concentration of 2.5 μM nanoparticle and 16.7% polymer in solution. The same subconjunctival injection procedure as those described in Section 2.2 was used except that the injection solution and microsyringe were kept on ice before the injection. Whole-body fluorescence imaging was performed and in this study, images were obtained at 0, 4, 9, 12, 24, 48, and 72 h after the injection and the data were analyzed as described in Section 2.3. Additional control experiments to compare the fluorescence signals of the hydrogels (without pRNA-Pent) to that of the background and to examine possible interference of the hydrogels to the fluorescence signal of the RNA nanoparticle were also performed by imaging the hydrogels in clear centrifuge tubes.

2.7. Distribution and retention of pRNA-Tri, pRNA-Sqr, and pRNA-Pent in the eye after subconjunctival injection with AK97

As AK97 showed the longest pRNA retention in the pharmacokinetics study among the polymer systems tested (see Section 3.3), AK97 was selected to examine the effect of thermosensitive polymer on the retention of pRNA-Tri, pRNA-Sqr, and pRNA-Pent of 10 nm edge length in the eye after subconjunctival injection. In the experiments, the same concentration of pRNA (2.5 μM) as in the distribution study in Section 2.4 was used except that the time points to sacrifice the animals were 24, 36, and 48 h after the injection of the RNA nanoparticles in AK97. The distribution of RNA nanoparticles in the eye was determined as described in Section 2.4. Results were analyzed by comparing the data of the RNA nanoparticles in AK97 with those in PBS in the injection at the same time points.

2.8. Statistical analysis

The data obtained in the present study were presented as mean and standard error of the mean (SEM). Regression analyses were performed using LINEST function in Microsoft Excel (Redmond, WA) and the results were presented as mean and standard error (SE). Statistical analyses were conducted using one-way ANOVA, and difference of $p < 0.05$ was considered statistically significant.

3. Results

3.1. Pharmacokinetics of pRNA-Tri, pRNA-Sqr and pRNA-Pent after subconjunctival injection in vivo

Figure 1 shows the atomic force microscopy (AFM) images of the RNA nanoparticles and summarizes the characteristics and sizes of these nanoparticles. The clearance of RNA nanoparticles from the eye after subconjunctival injection of the nanoparticles in PBS was investigated using whole-body imaging (Fig. 2). The percentage signal intensity at a time

point to that of zero time point was calculated and plotted against time. Figure 2 insert shows a representative whole-body image of the eye after subconjunctival injection of the RNA nanoparticle. A decrease in fluorescence signals of pRNA-Tri, pRNA-Sqr, and pRNA-Pent in the eye over time was observed, which could be described as biphasic first-order elimination. For example, only approximately 5–10% of the fluorescence signals from pRNA-Tri, pRNA-Sqr, and pRNA-Pent of 10 nm edge length and pRNA-Sqr of 20 nm edge length remained in the eye at 24 h after the injection. Also shown in the figure was the results from ds-RNA and Alexa-647 dye as the controls. The fluorescence signals associated with ds-RNA and the dye approached the background level within 10 h after the injection. The signals of the dye were significantly lower ($p < 0.05$) than that of the ds-RNA when compared at all time points, and the signals of both ds-RNA and the dye were significantly lower ($p < 0.05$) than those of the RNA nanoparticles. In the first 24 h after the injection, pRNA-Pent had significantly higher signals ($p < 0.05$) than those of pRNA-Tri and pRNA-Sqr when compared at the same time points. The pRNA-Sqr of 5 nm edge length had significantly lower signals than those of pRNA-Tri, pRNA-Sqr, and pRNA-Pent of 10 nm edge length and pRNA-Sqr of 20 nm edge length at all time points. No significant difference was observed between the signal levels of pRNA-Tri and pRNA-Sqr of 10 nm and 20 nm edge lengths at all time points ($p > 0.05$). Table 1 summarizes the apparent elimination rate constants of the fast elimination phase in the first 6 h for the dye, ds-RNA, and RNA nanoparticles in the eye after subconjunctival injection under the assumption of first order clearance (Eq. 1). The elimination rate constants of ds-RNA and the dye were significantly higher than those of the RNA nanoparticles, with the dye that was the smallest in molecular size showing the highest rate constant. This demonstrates the influence of the sizes of the nanoparticles upon their clearance from the eye.

3.2. Distribution of pRNA-Tri, pRNA-Sqr, and pRNA-Pent in mouse eye after subconjunctival injection in microscopy study

Figure 3 summarizes the percent of cells (relative number of cells to total cells stained by DAPI) that are associated with pRNA-Tri, pRNA-Sqr, or pRNA-Pent of 10 nm edge length in the dissected eye tissues when the mice were sacrificed at 6, 12, 24, 36, and 48 h after subconjunctival injection of the nanoparticles in PBS. The representative images of RNA nanoparticle in the conjunctiva, cornea, retina, and sclera after the injection and the results of pRNA-X, ds-RNA, and Alexa-647 dye are also provided for comparison (Fig. 3). No ds-RNA and dye were found in the cells of the eye tissues after subconjunctival injection under the conditions in the present study. pRNA-X was found up to 12 h in the cells of the cornea, retina, and sclera, and pRNA-Tri, pRNA-Sqr, and pRNA-Pent were found in the three tissues up to 36 h after the injection. At the 6-h time point, significantly higher levels ($p < 0.05$) of pRNA-Tri and pRNA-Sqr were found in the cornea compared to pRNA-Pent. At 24 h and 36 h, pRNA-Pent had significantly higher levels ($p < 0.05$) in the cornea, retina, and sclera than pRNA-Tri and pRNA-Sqr. The 48-h microscopy images had very low levels of pRNA-Pent in the conjunctiva and sclera, while pRNA-Tri and pRNA-Sqr were not detected in the eye tissues (cornea, conjunctiva, sclera, and retina). The microscopy data show relatively fast nanoparticle clearance from the eye tissues, which is consistent with the whole-body imaging results observed in Section 3.1.

In addition to the fluorescence microscopy study of the dissected eyes after subconjunctival injection, the uptake of the RNA nanoparticles into cornea, sclera, and retina cells was also examined *ex vivo* using eye tissues extracted from mice in a separate study (unpublished data). The objective was to delineate the effect of cellular uptake of the nanoparticles from that of subconjunctival delivery and clearance in the eye. In the experiment, freshly dissected eye tissues were equilibrated in 1 μM pRNA-Tri, pRNA-Sqr, and pRNA-Pent in cell culture medium (RPMI-1640 with 10% FBS) at 37°C in an incubator for 3 or 6 h. Tissues without nanoparticle equilibration were the control. After equilibration, the tissues were rinsed with PBS, fixed by 4% PFA, stained by DAPI, mounted on microscope slides, and examined with apotome fluorescence microscopy as described in the whole mount microscopy procedure in the present study. The results show no significant difference between the uptake of pRNA-Tri, pRNA-Sqr, and pRNA-Pent into the cells in the tissues. This suggests that the cellular uptake efficiencies of the nanoparticles were not the major cause of the different results observed among the RNA nanoparticles in Fig. 3.

3.3. Pharmacokinetics of pRNA-Pent after subconjunctival injection with thermosensitive PLGA-PEG-PLGA polymers

The liquid-to-gel transition temperatures were approximately 20°C, 30°C, and 25°C, and the gel-to-precipitation temperatures were approximately 30°C, 45°C, and 35°C for the sol-gel systems of 16.7% AK24, 16.7% AK97, and 1:1 mixture of AK24 and AK97 at total concentration of 16.7%, respectively. The liquid-to- gel transition temperatures of the triblock copolymers are expected to increase with increasing PEG length and decreasing LA:GA ratio [15, 21]. Although AK97 has a higher LA:GA ratio than AK24, AK97 has longer PEG and therefore higher transition temperature than AK24. The PLGA-PEG-PLGA systems were selected in this study to cover the temperature range that might be encountered in the subconjunctival space and around the eye in mice under anesthesia; the concentration and type of polymers were selected based on their liquid-to-gel transition temperatures. The temperature on the eye surface in the cul-de-sac under the eyelid measured using an ultrafine flexible temperature microprobe (0.009 inch diameter) was approximately 30–31°C in mice under anesthesia (unpublished data). This value is around 3–5°C lower than the surface temperature of human eye [22, 23]. In addition, the liquid phase of AK97 has higher viscosity than that of AK24, and the gel phase of AK24 has higher peak viscosity than that of AK97 according to physical observation and data from the manufacturer. Both the transition temperatures and viscosities of the polymer systems could affect the clearance of the RNA nanoparticles in the subconjunctival pocket after the injection.

Figure 4 presents the percent fluorescence intensity versus time profiles of the eye after subconjunctival injection of pRNA-Pent with the sol-gel polymers in the whole-body imaging study. Similar to the results in Fig. 2, the signal of the RNA nanoparticle decreased over time after the injection. In the presence of the polymers, the clearance of the nanoparticle from the eye was significantly slower ($p < 0.05$) than that without the polymers. AK97 provided the highest signal levels ($p < 0.05$) of pRNA-Pent among the sol-gel systems studied when compared at the same time points of the latter part of the profiles after the injection. At 3 days after the pRNA-Pent injection with AK97, up to 20% signal of the nanoparticle remained in the eye. Under the assumption of first order clearance, the apparent

elimination rate constants of pRNA-Pent with the polymers were calculated using Eq. 1, and the results are presented in Table 1. The polymers increased the residence time of pRNA-Pent in the eye and the elimination rate constants was reduced by 2–4 times. To examine the effects of the polymers on RNA nanoparticle delivery to the cells in the eye tissues, fluorescence microscopy study was performed with AK97 (see Section 3.4).

3.4. Distribution and retention of pRNA-Tri, pRNA-Sqr, and pRNA-Pent in the eye after subconjunctival injection with AK97

Figure 5 shows the distribution of pRNA-Tri, pRNA-Sqr, and pRNA-Pent in conjunctiva, cornea, retina, and sclera tissues after subconjunctival injection of the pRNA with 16.7% AK97. The data show that AK97 could increase the percent of cell internalization of the pRNA in the tissues at 24-48 h after the injection; the levels of pRNA in conjunctiva, cornea, retina, and sclera tissues with AK97 were significantly higher ($p < 0.05$) than those injected in PBS without the polymer, except pRNA-Tri in retina and sclera at 24 h and 36 h, pRNA-Tri in sclera at 48 h, and pRNA-Pent in cornea at 24 h (not statistically different from the PBS results). Similar to the PBS data (without the polymer), the figure also shows that the percent of cells associated to pRNA for pRNA-Pent with AK97 was significantly higher ($p < 0.05$) than those of pRNA-Tri and pRNA-Sqr with AK97, except in cornea (pRNA-Pent vs pRNA-Tri and pRNA-Pent vs pRNA-Sqr) and retina (pRNA-Pent vs pRNA-Sqr) at 24 h.

4. Discussion

4.1. Triangular, square, and pentagonal RNA nanoparticles in ocular delivery

Ocular delivery of RNA nanoparticles pRNA-3WJ and pRNA-X via subconjunctival administration was examined in a previous study [14]. The present study investigated five new RNA nanoparticles (pRNA-Tri, pRNA-Sqr, and pRNA-Pent of 10 nm edge length and pRNA-Sqr of 5 and 20 nm edge lengths) derived from the non-toxic and thermodynamically stable pRNA 3WJ motif as the building block. The characteristics of these RNA nanoparticles for drug delivery have been previously investigated [7, 24]. Briefly, these RNA nanoparticles are planar polygons of triangle, square, and pentagon with the pRNA 3WJ motif located at their vertices. The edge lengths (length of each side) of the polygon were 5, 10, and 20 nm. The molecular weights of pRNA-Tri, pRNA-Sqr, and pRNA-Pent of 10 nm edge length and pRNA-Sqr of 20 nm edge length were approximately 69–144 kDa, and therefore the RNA polygons were larger than pRNA-3WJ and pRNA-X. These RNA polygons could serve as multivalent nanocarriers with functional modules for targeting, therapeutic, and detection at their vertices. The RNA nano-scaffolds were constructed by one-step self-assembly, and their sizes and shapes were shown to be important factors for the induction of immunostimulatory processes when they harbored different numbers of unmethylated cytosine-phosphate-guanine oligodeoxynucleotides (CpG ODN) as their payload [7]. Particularly, the targeting and therapeutic modules can be nucleotide sequences extended from the 3WJ structures of the RNA nanoparticles. Possible therapeutic modules are aptamers that target the vascular endothelial growth factor (anti-VEGF aptamer) and other transcription factors for the treatment of eye diseases.

Intravitreal injection is an effective method for drug delivery to the posterior segment of the eye, e.g., to the retina. However, frequent intravitreal injections can lead to severe adverse effects. Effective drug delivery to the retina by an alternative route without the perforation of the globe has been a difficult task. Subconjunctival injection is less invasive than intravitreal injection and carries less risk of severe adverse effects. Subconjunctival injection of nanoparticles can provide sustained delivery of small molecules to the anterior and posterior eye tissues [25], but cell internalization of macromolecules or nanoparticles in the retinal tissues could only be achieved by invasive intraocular drug delivery methods [26–28]. The distribution and clearance of pRNA-3WJ and pRNA-X have been reported previously, and the delivery of pRNA-X into the cells of the retina via subconjunctival injection has been demonstrated in an animal model [14]. This suggests the potential utility of RNA nanoparticles for ocular delivery of oligonucleotides, such as siRNA and miRNA, for cell transfection and targeted gene delivery to provide treatment of posterior eye diseases [29–32]. The present study examined the effects of RNA nanoparticle sizes on subconjunctival delivery using pRNA-Tri, pRNA-Sqr, and pRNA-Pent.

4.2. Ocular clearance of RNA nanoparticles

One of the hindering factors in the development of ocular drug delivery systems is the lack of understanding of ocular pharmacokinetics due to the complicated anatomy and physiology of the eye [33]. For example, the mechanisms of ocular delivery of nanoparticles and their distribution and elimination in the eye are not completely understood, and effective treatment of eye diseases using nanoparticles would require this information [34]. In the present whole-body fluorescence imaging study, the clearance of the RNA nanoparticles from the eye was investigated. The trend of increasing nanoparticle retention in the eye with increasing particle sizes from pRNA-Tri to pRNA-Pent could be attributed to the decrease in nanoparticle diffusion, tissue permeation, and clearance with an increase in the nanoparticle size. For comparison, the experiments conducted with Alexa-647 dye showed significantly faster clearance than the RNA nanoparticles. The half-life of the dye was approximately 0.6 h, which is consistent with those of small molecule clearance from the subconjunctival pocket in previous studies [35, 36]. The half-lives of the RNA nanoparticles were 2–3 h, significantly longer than that of the dye and consistent with the size-dependent clearance of subconjunctival nanoparticles observed previously [34, 37]. The short half-life of ds-RNA (approximately 1 h) compared with those of the RNA nanoparticles in the present study is also consistent with the size-dependent clearance relationship of molecules/particles in subconjunctival delivery. In addition, the half-life of ds-RNA in the present study was similar to those of ds-RNA, pRNA-3WJ, and pRNA-X (approximately 1 to 1.5 h) investigated at a higher concentration previously [14]; this is consistent with the half-lives of first-order kinetics that are concentration independent. It should be noted that the RNA nanoparticles examined in the present study did not contain any drugs, therapeutic modules, or targeting agents. When high molecular weight modules such as macromolecule drugs are incorporated in these nanoparticles, the sizes and shapes of the nanoparticles could be altered considerably. This could affect the behaviors and pharmacokinetics of the nanoparticles in the eye. Future studies are needed to investigate these effects.

Although the RNA nanoparticles of polygons had longer residence time in the eye than the dye (i.e., small molecules), their half- lives were still relatively short, resulting in less than 10% of the nanoparticles remaining in the eye after 24 h. This fast ocular clearance after subconjunctival administration is likely related to the dynamic barriers of blood and lymphatic circulations, and suggests that frequent injections are required to maintain the concentration of the nanoparticles (or cell internalization) in the eye tissues. In the presence of the thermosensitive sol-gel systems, the half-lives of the fluorescence signals of the RNA nanoparticle in the eye increased significantly after subconjunctival injection. The polymer solutions were liquid at cool temperature and became a gel when the temperature increased to body surface temperature above their transition temperatures; AK24, AK97, and the mixture of AK24 and AK97 had transition temperatures of 20–30°C. In addition, the polymer solutions had higher viscosity than PBS. These polymers are therefore expected to increase the retention times of the nanoparticles for their delivery into the eye. Thermosensitive PLGA-PEG-PLGA polymers have been investigated in subconjunctival delivery previously [18]. This type of polymers has also been used as materials in corneal wound healing [38] and other ocular delivery applications [16, 39]. In addition to the triblock polymers, multiblock polymers have also been developed for ocular delivery such as to improve the physical characteristics of the thermosensitive systems and prolong drug release after intravitreal and intracameral injections [40–42]. Only triblock PLGA-PEG-PLGA polymers were studied in the present project as the first attempt to improve subconjunctival delivery of the RNA nanoparticles. In the present whole-body imaging study, the thermosensitive polymers enhanced the retention of the RNA nanoparticles in the eye after subconjunctival injection, with AK97 providing the most significant effect. The polymers increased the half-lives of pRNA-Pent in the eye by 2–4 times and up to 20% of the nanoparticles remained in the eye after 3 days.

4.3. Ocular distribution and cell internalization of RNA nanoparticles

The results in the present distribution microscopy study were compared with those of Alexa-647 dye, ds-RNA, pRNA-3WJ, and pRNA-X in a previous study [14]. Consistent with the previous results, no Alexa-647 dye was found in the cells of the eye tissues after subconjunctival injection in the present study. It should be noted that the RNA nanoparticle concentration (injection solution) used in this study was lower than that in the previous study (20X difference). Because of the difference in concentrations, pRNA-X experiment at 6 h was repeated in the present study using the concentration in the previous study to ensure consistency in our experimental techniques, and the present pRNA-X result was essentially the same as that in the previous study (data not shown). Although lower pRNA-X concentration was used in the present study, the results at these two concentrations show the same pRNA-X distribution behavior in the eye. Different from the previous ds-RNA result, ds-RNA was not observed in the cells of the eye tissues in the present study except in the conjunctiva at 6 h. The difference between the ds-RNA results in the present and previous studies can be attributed to the lower ds-RNA concentration used in the present study.

In the previous study of RNA nanoparticles, only pRNA-X was observed in the cells of the retina after subconjunctival injection, and no RNA nanoparticles remained in the retinal cells at 12 h [14]. Despite the short retention time, the ability of pRNA-X to penetrate the globe

and provide cell internalization is significant considering the challenges to deliver nanoparticles across the transscleral barrier into the cells in the retina via subconjunctival injection. For the RNA nanoparticles in the present microscopy study, although the early time results of the RNA nanoparticles were not significantly different from each other, pRNA-Pent provided significantly longer retention in the corneal, retinal, and scleral cells compared with the other RNA nanoparticles. This suggests that the sizes of the RNA nanoparticles could be a major factor influencing the delivery and/or clearance of the nanoparticles in the eye tissues. Another possible explanation is the larger RNA nanoparticles being more effectively taken up by the conjunctival, corneal, retinal, and scleral cells, similar to the behavior observed in macrophages [7]; uptake of pRNA nanoparticles into macrophages and tumor cells was observed in cell culture *in vitro* and animals *in vivo* previously [7, 43]. This could lead to longer retention for the larger nanoparticles and the observed slower clearance from the eye tissues. RNA stability could also affect pRNA clearance. However, pRNA nanoparticles were found to be stable in chemical and biological environments such as in serum for at least 14 h [6, 7, 9], so it is unlikely that the difference in pRNA degradation would contribute significantly to the observed difference in pRNA clearance.

In spite of the longer retention due to the sizes of the nanoparticles, no nanoparticles could be found in the cells of the eye tissues (cornea, conjunctiva, sclera, and retina) at 48 h after subconjunctival injection in PBS, consistent with the fast clearance observed in the whole-body imaging study. While the prolonged retention of pRNA-Tri, pRNA-Sqr, and pRNA-Pent compared to pRNA-X could lead to better outcome in ocular delivery, this improvement is not sufficient, and frequent subconjunctival injections are likely required for drug delivery in long treatment. The use of the thermosensitive sol-gel system increased the residence time of the RNA nanoparticles in the cells of the eye after subconjunctival injection. Similar to the whole-body imaging results, the effects of the thermosensitive polymer are statistically significant and considerable amounts of RNA nanoparticles were found to be associated with the cells at 48 h after subconjunctival injection. However, the clearance of the nanoparticles from the eye was still fast even with the sol-gel sustained delivery system when compared to the long treatment time (e.g., months) required for chronic posterior eye diseases.

5. Conclusions

Subconjunctival delivery of RNA nanoparticles that have different sizes and shapes (pRNA-Tri, pRNA-Sqr, and pRNA-Pent of 10 nm edge length and pRNA-Sqr of 5 and 20 nm edge lengths) was evaluated in mice and compared to the previous results of pRNA-X for their behaviors in ocular delivery. These nanoparticles also provided the opportunity to investigate the influence of nanoparticle sizes on the distribution and clearance of nanoparticles in the eye after subconjunctival injection. The present study showed that the nanoparticles of larger particle sizes had slower clearance. The decrease of the RNA nanoparticle signals in the eye followed biphasic first-order clearance. Cell internalization of the nanoparticles was observed in the eye tissues (e.g., cornea and retina) via subconjunctival delivery. Unlike pRNA-X, the larger nanoparticles pRNA-Tri, pRNA-Sqr, and pRNA-Pent stayed in the cells in the eye for up to 24 h. The PLGA-PEG-PLGA sol-gel systems (AK97, AK24, and 1:1

mixture of AK24 and AK97) prolonged the residence time of the nanoparticles in the eye. AK97 provided the longest nanoparticle retention in the eye among the systems studied and increased the half-lives of pRNA-Pent by 2–4 times after subconjunctival injection in the animal model.

Acknowledgments

The authors thank Dr. Winston W-Y. Kao and Dr. Mindy K. Call for providing the AxioCam Observer Z1 microscope and their help in the microscopy study; Kathleen LaSance at the Vontz Core Imaging Laboratory (VCIL), University of Cincinnati, for her help in the whole-body imaging study; Mario Vieweger, Congcong Xu, and Apipa Wanasathop for their help in the laboratories; and Dr. Tanansait Ngawhirunpat and Dr. Thomas W.Y. Lee for helpful discussion.

Funding

This research was supported in part by NIH grant R21EY024409, the Thailand Research Fund (TRF) through the Royal Golden Jubilee Ph.D. Program to Charoenputtakun, and NCI grant U01CA207946 to Guo.

References

1. Guo P. The emerging field of RNA nanotechnology. Nat Nanotechnol. 2010; 5:833–842. [PubMed: 21102465]
2. Guo P, Haque F, Hallahan B, Reif R, Li H. Uniqueness, advantages, challenges, solutions, and perspectives in therapeutics applying RNA nanotechnology. Nucleic Acid Ther. 2012; 22:226–245. [PubMed: 22913595]
3. Kim DH, Rossi JJ. Strategies for silencing human disease using RNA interference. Nat Rev Genet. 2007; 8:173–184. [PubMed: 17304245]
4. Guo P, Zhang C, Chen C, Garver K, Trottier M. Inter-RNA interaction of phage phi29 pRNA to form a hexameric complex for viral DNA transportation. Mol Cell. 1998; 2:149–155. [PubMed: 9702202]
5. Haque F, Shu D, Shu Y, Shlyakhtenko LS, Rychahou PG, Evers BM, Guo P. Ultrastable synergistic tetravalent RNA nanoparticles for targeting to cancers. Nano Today. 2012; 7:245–257. [PubMed: 23024702]
6. Shu D, Shu Y, Haque F, Abdelmawla S, Guo P. Thermodynamically stable RNA three-way junction for constructing multifunctional nanoparticles for delivery of therapeutics. Nat Nanotechnol. 2011; 6:658–667. [PubMed: 21909084]
7. Khisamutdinov EF, Li H, Jasinski DL, Chen J, Fu J, Guo P. Enhancing immunomodulation on innate immunity by shape transition among RNA triangle, square and pentagon nanovehicles. Nucleic Acids Res. 2014; 42:9996–10004. [PubMed: 25092921]
8. Shu Y, Pi F, Sharma A, Rajabi M, Haque F, Shu D, Leggas M, Evers BM, Guo P. Stable RNA nanoparticles as potential new generatio n drugs for cancer therapy. Adv Drug Deliv Rev. 2014; 66:74–89. [PubMed: 24270010]
9. Jasinski DL, Khisamutdinov EF, Lyubchenko YL, Guo P. Physicochemically tunable polyfunctionalized RNA square architecture with fluorogenic and ribozymatic properties. ACS Nano. 2014; 8:7620–7629. [PubMed: 24971772]
10. Abdelmawla S, Guo S, Zhang L, Pulukuri SM, Patankar P, Conley P, Trebley J, Guo P, Li QX. Pharmacological characterization of chemically synthesized monomeric phi29 pRNA nanoparticles for systemic delivery. Mol Ther. 2011; 19:1312–1322. [PubMed: 21468004]
11. Urtti A. Challenges and obstacles of ocular pharmacokinetics and drug delivery. Adv Drug Deliv Rev. 2006; 58:1131–1135. [PubMed: 17097758]
12. Gaudana R, Jwala J, Boddu SH, Mitra AK. Recent perspectives in ocular drug delivery. Pharm Res. 2009; 26:1197–1216. [PubMed: 18758924]
13. Lee SS, Robinson MR. Novel drug delivery systems for retinal diseases. A review. Ophthalmic Res. 2009; 41:124–135. [PubMed: 19321933]

14. Feng L, Li SK, Liu H, Liu CY, LaSance K, Haque F, Shu D, Guo P. Ocular delivery of pRNA nanoparticles: distribution and clearance after subconjunctival injection. Pharm Res. 2014; 31:1046–1058. [PubMed: 24297069]
15. Jeong B, Kim SW, Bae YH. Thermosensitive sol-gel reversible hydrogels. Adv Drug Deliv Rev. 2002; 54:37–51. [PubMed: 11755705]
16. Gao Y, Sun Y, Ren F, Gao S. PLGA-PEG-PLGA hydrogel for ocular drug delivery of dexamethasone acetate. Drug Dev Ind Pharm. 2010; 36:1131–1138. [PubMed: 20334543]
17. Chen S, Pieper R, Webster DC, Singh J. Triblock copolymers: synthesis, characterization, and delivery of a model protein. Int J Pharm. 2005; 288:207–218. [PubMed: 15620860]
18. Lee, TWY. PhD Thesis. University of Wisconsin; 2003. Drug delivery to the posterior segment of the eye by subconjunctival injection.
19. Zhang W, Zhao J, Chen L, Urbanowicz MM, Nagasaki T. Abnormal epithelial homeostasis in the cornea of mice with a destrin deletion. Mol Vis. 2008; 14:1929–1939. [PubMed: 18958303]
20. Liu H, Zhang J, Liu CY, Wang IJ, Sieber M, Chang J, Jester JV, Kao WW. Cell therapy of congenital corneal diseases with umbilical mesenchymal stem cells: lumican null mice. PLoS One. 2010; 5:e10707. [PubMed: 20502663]
21. Shim MS, Lee HT, Shim WS, Park I, Lee H, Chang T, Kim SW, Lee DS. Poly(D,L-lactic acid-co-glycolic acid)-b-poly(ethylene glycol)-b-poly (D,L-lactic acid-co-glycolic acid) triblock copolymer and thermoreversible phase transition in water. J Biomed Mater Res. 2002; 61:188–196. [PubMed: 12007198]
22. Sniegowski M, Erlanger M, Velez-Montoya R, Olson JL. Difference in ocular surface temperature by infrared thermography in phakic and pseudophakic patients. Clin Ophthalmol. 2015; 9:461–466. [PubMed: 25834383]
23. Sodi A, Matteoli S, Giacomelli G, Finocchio L, Corvi A, Menchini U. Ocular surface temperature in age-related macular degeneration. J Ophthalmol. 2014; 2014:281010. [PubMed: 25436140]
24. Jasinski DL, Li H, Guo P. The effect of size and shape of RNA nanoparticles on biodistribution. in press.
25. Pan Q, Xu Q, Boylan NJ, Lamb NW, Emmert DG, Yang JC, Tang L, Heflin T, Alwadani S, Eberhart CG, Stark WJ, Hanes J. Corticosteroid-loaded biodegradable nanoparticles for prevention of corneal allograft rejection in rats. J Control Release. 2015; 201:32–40. [PubMed: 25576786]
26. Andrieu-Soler C, Halhal M, Boatright JH, Padove SA, Nickerson JM, Stodulkova E, Stewart RE, Ciavatta VT, Doat M, Jeanny JC, de Bizemont T, Sennlaub F, Courtois Y, Behar-Cohen F. Single-stranded oligonucleotide- mediated in vivo gene repair in the rd1 retina. Mol Vis. 2007; 13:692–706. [PubMed: 17563719]
27. Bejjani RA, BenEzra D, Cohen H, Rieger J, Andrieu C, Jeanny JC, Gollomb G, Behar-Cohen FF. Nanoparticles for gene delivery to retinal pigment epithelial cells. Mol Vis. 2005; 11:124–132. [PubMed: 15735602]
28. Bourges JL, Gautier SE, Delie F, Bejjani RA, Jeanny JC, Gurny R, BenEzra D, Behar-Cohen FF. Ocular drug delivery targeting the retina and retinal pigment epithelium using polylactide nanoparticles. Invest Ophthalmol Vis Sci. 2003; 44:3562–3569. [PubMed: 12882808]
29. Ng EW, Shima DT, Calias P, Cunningham ET Jr, Guyer DR, Adamis AP. Pegaptanib, a targeted anti-VEGF aptamer for ocular vascular disease. Nat Rev Drug Discov. 2006; 5:123–132. [PubMed: 16518379]
30. Nguyen QD, Schachar RA, Nduaka CI, Sperling M, Basile AS, Klamerus KJ, Chi-Burris K, Yan E, Paggiarino DA, Rosenblatt I, Aitchison R, Erlich SS. Dose-ranging evaluation of intravitreal siRNA PF-04523655 for diabetic macular edema (the DEGAS study). Invest Ophthalmol Vis Sci. 2012; 53:7666–7674. [PubMed: 23074206]
31. Henry SP, Miner RC, Drew WL, Fitchett J, York-Defalco C, Rapp LM, Levin AA. Antiviral activity and ocular kinetics of antisense oligonucleotides designed to inhibit CMV replication. Invest Ophthalmol Vis Sci. 2001; 42:2646–2651. [PubMed: 11581212]
32. Hennig R, Goepferich A. Nanoparticles for the treatment of ocular neovascularizations. Eur J Pharm Biopharm. 2015
33. Ghate D, Edelhauser HF. Ocular drug delivery. Expert Opin Drug Deliv. 2006; 3:275–287. [PubMed: 16506953]

34. Amrite AC, Kompella UB. Size-dependent disposition of nanoparticles and microparticles following subconjunctival administration. J Pharm Pharmacol. 2005; 57:1555–1563. [PubMed: 16354399]

35. Kim SH, Csaky KG, Wang NS, Lutz RJ. Drug elimination kinetics following subconjunctival injection using dynamic contrast-enhanced magnetic resonance imaging. Pharm Res. 2008; 25:512–520. [PubMed: 17674155]

36. Li SK, Molokhia SA, Jeong EK. Assessment of subconjunctival delivery with model ionic permeants and magnetic resonance imaging. Pharm Res. 2004; 21:2175–2184. [PubMed: 15648248]

37. Amrite AC, Edelhauser HF, Singh SR, Kompella UB. Effect of circulation on the disposition and ocular tissue distribution of 20 nm nanoparticles after periocular administration. Mol Vis. 2008; 14:150–160. [PubMed: 18334929]

38. Pratoomsoot C, Tanioka H, Hori K, Kawasaki S, Kinoshita S, Tighe PJ, Dua H, Shakesheff KM, Rose FR. A thermoreversible hydrogel as a biosynthetic bandage for corneal wound repair. Biomaterials. 2008; 29:272–281. [PubMed: 17976717]

39. Duvvuri S, Janoria KG, Pal D, Mitra AK. Controlled delivery of ganciclovir to the retina with drug-loaded Poly(d,L-lactide-co-glycolide) (PLGA) microspheres dispersed in PLGA-PEG-PLGA Gel: a novel intravitreal delivery system for the treatment of cytomegalovirus retinitis. J Ocul Pharmacol Ther. 2007; 23:264–274. [PubMed: 17593010]

40. Bates FS, Hillmyer MA, Lodge TP, Bates CM, Delaney KT, Fredrickson GH. Multiblock polymers: panacea or Pandora's box? Science. 2012; 336:434–440. [PubMed: 22539713]

41. Patel SP, Vaishya R, Pal D, Mitra AK. Novel pentablock copolymer-based nanoparticulate systems for sustained protein delivery. AAPS PharmSciTech. 2015; 16:327–343. [PubMed: 25319053]

42. Schaefer E, Smith SM, Salmon J, Abbaraju S, Amin R, Weiss S, Grau U, Velagaleti P, Gilger B. Evaluation of Intracameral Pentablock Copolymer Thermosensitive Gel for Sustained Drug Delivery to the Anterior Chamber of the Eye. J Ocul Pharmacol Ther. 2017; 33:353–360. [PubMed: 28300477]

43. Zhang Y, Leonard M, Shu Y, Yang Y, Shu D, Guo P, Zhang X. Overcoming Tamoxifen Resistance of Human Breast Cancer by Targeted Gene Silencing Using Multifunctional pRNA Nanoparticles. ACS Nano. 2017; 11:335–346. [PubMed: 27966906]

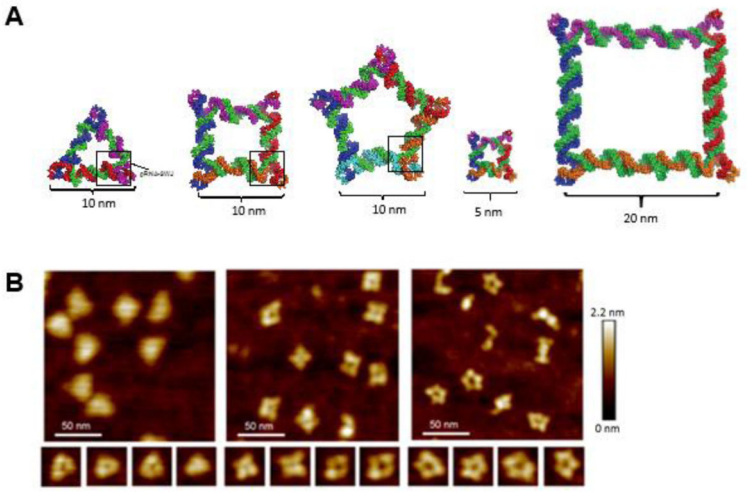

C

	ds-RNA	pRNA-X	pRNA-Tri 10 nm	pRNA-Sqr 5 nm	pRNA-Sqr 10 nm	pRNA-Sqr 20 nm	pRNA-Pent 10 nm
Total number of nucleotides (nt)	32nt	68nt	210nt	151nt	280nt	436nt	350nt
Length of external strand	--- [a]	--- [a]	48nt	30nt	48nt	65nt	48nt
Length of internal strand	--- [a]	--- [a]	66nt	31nt	88nt	176nt	110nt
Molecular weight (kDa)	11	22	69	50	92	144	116

Fig. 1.

Structural details of RNA polygons. **(A)** Schematic images of pRNA-Tri, pRNA-Sqr, and pRNA-Pent of 10 nm edge length (length along each edge) and pRNA-Sqr of 5 and 20 nm edge lengths. **(B)** AFM images of pRNA-Tri, pRNA-Sqr, and pRNA-Pent of 10 nm edge length. **(C)** Size details of RNA polygons. Data obtained from [7]. [a] Not applicable.

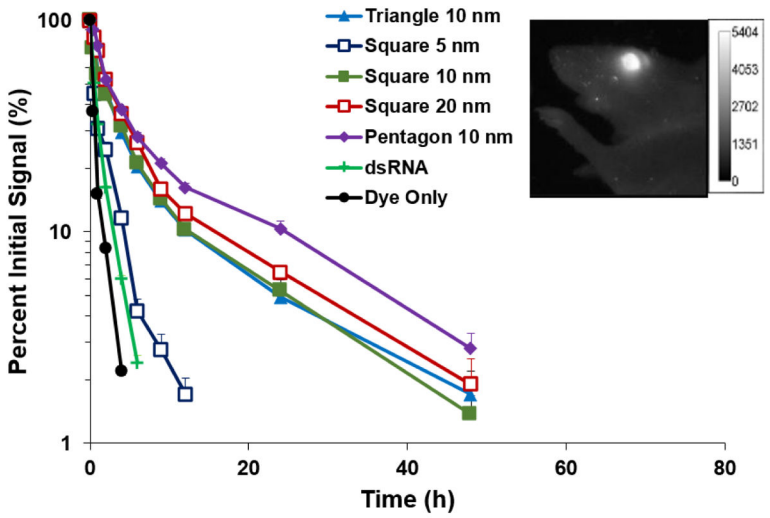

Fig. 2.

Relative signal versus time after subconjunctival injection in mouse eye *in vivo* of pRNA-Tri, pRNA-Sqr, and pRNA-Pent of 10 nm edge length and pRNA-Sqr of 5 and 20 nm edge lengths in PBS. Relative signal was calculated as the percent of signal at the time point to that at time $t = 0$. Mean ± SEM (n = 3–5; except for pRNA-Sqr 10 nm, n = 9). Figure insert: representative whole-body image of the eye at 9 h after subconjunctival injection of pRNA-Pent on a mouse *in vivo*.

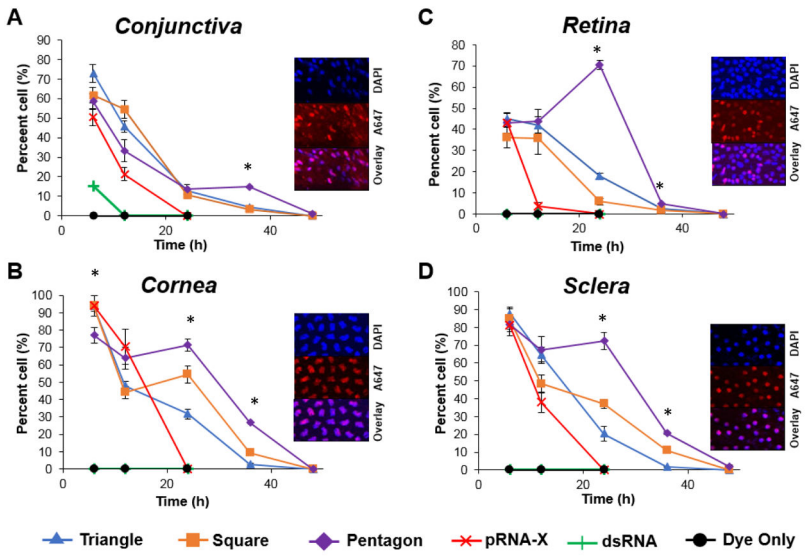

Fig. 3.

Percent of cells with detectable pRNA-Tri, pRNA-Sqr, pRNA-Pent, and pRNA-X in **(A)** conjunctiva, **(B)** cornea, **(C)** retina, and **(D)** sclera in mice versus time after subconjunctival injection (mean ± SEM, n = 3–4). The corneal cell count is of the corneal endothelium, and that of sclera is the RPE side of the sclera. * indicates $p < 0.05$ when comparing pRNA-Pent to other pRNA. Figure inserts: representative images of RNA nanoparticle (pRNA-Tri) delivered to the cells in the respective tissues at 6 h after the injection.

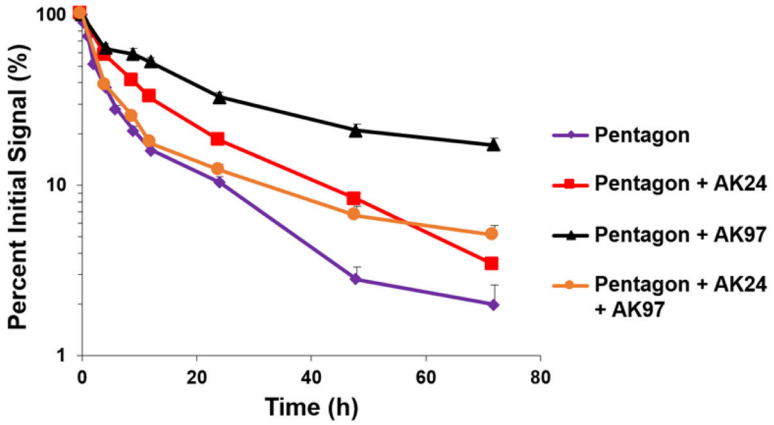

Fig. 4.

Relative signal of pRNA-Pent in mouse eye versus time after subconjunctival injection with thermosensitive polymers PLGA-PEG-PLGA (16.7% AK24, 16.7% AK97, or 16.7% 1:1 mixture of AK24 and AK97) *in vivo*. Relative signal was calculated as the percent of signal at the time point to that at time $t = 0$. Mean ± SEM (n = 4–5).

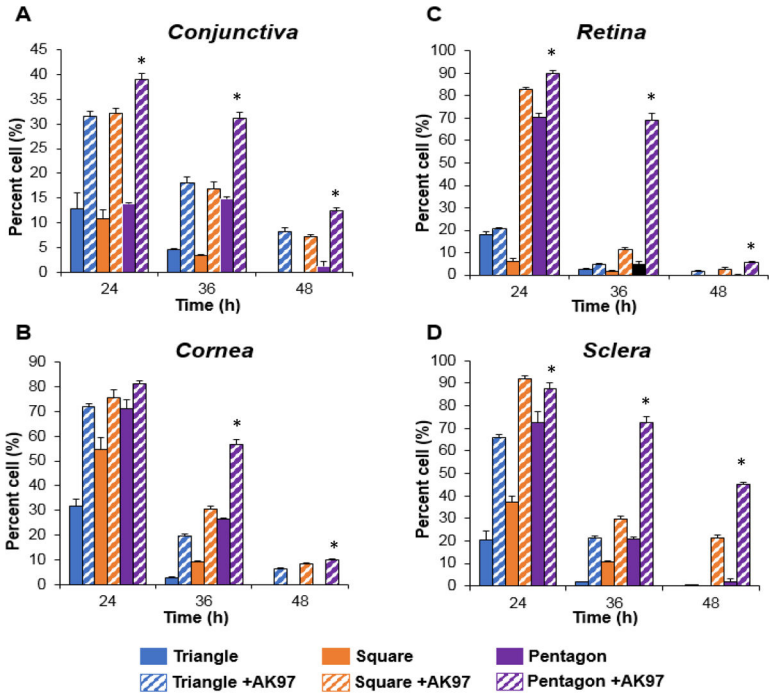

Fig. 5.

Percent of cells with detectable pRNA-Tri, pRNA-Sqr and pRNA-Pent in **(A)** conjunctiva, **(B)** cornea, **(C)** retina, and **(D)** sclera in mice versus time after subconjunctival injection in 16.7% polymer AK97. The corneal cell count is of the corneal endothelium, and that of sclera is the RPE side of the sclera. Mean ± SEM (n = 3–4). * indicates $p < 0.05$ when pRNA-Pent with AK97 data are compared to PBS.

Table 1

Apparent rate constants of the fast elimination phase of the biphasic clearance model for Alexa-647 dye, ds-RNA, pRNA-X, and pRNA-Tri, pRNA-Sqr, and pRNA-Pent of 10 nm edge length, and pRNA-Sqr of 5 nm and 20 nm edge lengths after subconjunctival injection with and without PLGA-PEG-PLGA copolymers.

Injection solution	k (h^{-1}) [a]
pRNA-Sqr 5 nm, PBS	0.47 ± 0.10
pRNA-Tri 10 nm, PBS	0.29 ± 0.04
pRNA-Sqr 10 nm, PBS	0.27 ± 0.05
pRNA-Sqr 20 nm, PBS	0.25 ± 0.02
pRNA-Pent 10 nm, PBS	0.25 ± 0.03
pRNA-X, PBS	0.47 [b]
ds-RNA, PBS	0.67 ± 0.08
Alexa-647, PBS	1.2 ± 0.3
pRNA-Pent 10 nm, AK24	0.10 ± 0.02
pRNA-Pent 10 nm, AK97	0.06 ± 0.02
pRNA-Pent 10 nm, AK24/AK97	0.14 ± 0.04

[a] Mean ± SE (n = 3–5).

[b] obtained from reference [14].